Electronic Supplementary Material (ESI) for Polymer Chemistry.

Supporting Information

Precise Polyethylene Derivatives Bearing Mesogenic Side-Chains: Delicate Self-Assembly Depending on Graft Density

Wen-Ying Chang,[a] Dong Shi,[a] Xu-Qiang Jiang,[a] Jia-Di Jiang,[a] Yang Zhao,[b] Xiang-Kui Ren,*[b] Shuang Yang,*[a] and Er-Qiang Chen,*

[a] Beijing National Laboratory for Molecular Sciences, Key Laboratory of Polymer Chemistry and Physics of Ministry of Education, Center for Soft Matter Science and Engineering, College of Chemistry, Peking University, Beijing, 100871, China. E-mail: eqchen@pku.edu.cn, yangshuang@iccas.ac.cn

[b] School of Chemical Engineering and Technology, Tianjin University, Tianjin, 300350, China. E-mail: renxiangkui@tju.edu.cn.

Table of Contents

Experimental Procedures

Materials

Dichloromethane (DCM), extra dry with molecular sieves, was purchased from 3A Chemicals (Shanghai, China). Grubbs 1st generation catalyst was purchased from Sigma-Aldrich. All the other chemicals were obtained from Energy Chemical (Shanghai, China) and used without further purification.

Instruments and measurements

^{1}H NMR (400 MHz) and ^{13}C NMR (100 MHz) spectra were recorded on a Bruker ARX400 spectrometer at room temperature using deuterated chloroform ($CDCl_3$) as the solvent and tetramethylsilane (TMS) as the internal standard. Elemental analysis was performed with an Elementar Vario EL instrument. Mass spectra were recorded on a Bruker Solarix XR mass spectrometer. Gel permeation chromatography (GPC) was carried out on a Waters 515 GPC instrument using THF as an eluent at a flow rate of 1.0 mL/min. The GPC calibration curve was obtained with linear polystyrene standards. Recycling preparative GPC was performed on a JAI LaboACE LC-5060 series equipped with two JAIGEL HR columns (2HR, 2.5 HR), a UV detector and a RI detector. Chloroform added 0.05% ethanol was used as eluent at a flow rate of 8.0 mL/min. The data was collected and processed with JAI Scan software.

Differential scanning calorimetry (DSC, TA Q1000 with a mechanical refrigerator) was utilized to study phase transitions of the polymers. The sample was encapsulated in a hermetically sealed aluminum pan, with a typical sample weight of 3-5 mg.

The mesophase textures were examined on a Nikon LV100N polarized optical microscope (POM) equipped with a Linkam THMSE600 Hot stage.

One-dimensional (1D) X-ray diffraction (XRD) powder experiments were performed on a Philips X'Pert Pro diffractometer with a 3 kW ceramic tube as the X-ray source (Cu Kα) and an X'celerator detector. The reflection peak positions were calibrated with silicon powder ($2\theta > 15°$) and silver behenate ($2\theta < 10°$). Background scattering was recorded and subtracted from the sample patterns. A temperature control unit (Anton Paar TCU 100) in conjunction with the diffractometer was utilized to study the structure evolution as a function of temperature. The heating and cooling rates in the WAXD experiments were 5 °C/min.

Two-dimensional (2D) XRD patterns of the oriented samples were recorded by employing Ganesha system (SAXSLAB, U.S) equipped with a multilayer focused Cu Kα radiation as the X-ray source (Genix3D Cu ULD) and a semiconductor detector (Pilatus 300 K, DECTRIS, Swiss). The scattering peak positions were calibrated with LaB_6 for the wide-angle region and silver behenate for the small-angle region, respectively. A Linkam TST350 stage was utilized to study the structure evolution as a function of temperature.

The chain conformation in **P*n***s was detected by using Fourier transform infrared spectrometer (FT-IR, nicolet is50, ThermoFisher) equipped with a polarizer. In a typical procedure, the **P*n***s were sheared by hand quickly at the temperatures slightly below their isotropic temperatures followed by quenching to room temperature. After annealing, the sheared polymer film was fixed on the KBr window to make sure that the shear direction is parallel or perpendicular to the polarizer.

Reconstruction of Relative Electron Density Map (EDM)

On the basis of XRD data, the reconstruction of relative electron density distribution in real space is carried out using the following formula for three-dimensional (3D) Fourier transformation:

$$\rho(x,y,z)-\rho_0=\sum_{hkl}F(hkl)\exp[i2\pi(hx+ky+lz)]$$

where ρ is the average electron density and x, y and z are the fractional coordinates of a point in the unit cell. F(hkl) is the complex structure factor and its modulus is related to the diffraction intensities *I*(*hkl*) by $|F(hkl)|=\sqrt{I(hkl)}$. Note that diffraction intensities need to be multiplicity corrected. In addition, the summation is executed over all possible integer combination of (*hkl*) except for (000).

If the lattice is chosen as centrosymmetric, the structure factor becomes real and is given by $F(hkl)=\pm|F(hkl)|$, with corresponding possible phase of 0 (+) or π (–). Then the electron density can be expressed as:

$$\rho(x,y,z)-\rho_0=\sum_{hkl}\pm\sqrt{I(hkl)}\cos[i2\pi(hx+ky+lz)]$$

If we consider a two-dimensional (2D) electron density distribution, then the third component *z* is absent and all calculations are performed in (*x*, *y*) space.

The EDMs were calculated using the suitable phase combinations for the corresponding reflections. In order to select the proper phases for the diffractions, we used a trial-and-error approach. All the possible phase combinations were used to reconstruct the EDMs. The “correct” map was then selected based on the quality of the map, aided by prior physical and chemical knowledge of the system.

For **P2**, to show the layer structure, the EDM was calculated based on the four low angle diffractions with the *q*-ratio of 1:2:3:4 in the XRD profile. The phases of the four diffractions are selected to be -, +, - and -.

For **P7**, to investigate the 3D ordered packing, the EDM was calculated using the seven diffractions of (101), (002), (112), (103), (301), (310), (400) in the XRD profile, with the phases of +, +, -, -, -, + and +, respectively.

For **P15**, to show the columnar LC structure, the EDM was calculated using the four low angle diffractions/scatterings in the XRD profile, of which the phases were selected to be +, -, + and -, respectively.

Molecular Mechanics Simulation

Molecular mechanics simulation was performed using Materials Studio software package 8.0 (Accelrys Software Inc.).

The single chain was built by linking 30 repeating units through head-to-tail arrangement with random connecting dihedral angles. Geometry optimization, Anneal and Dynamics calculation of single chains were carried out through the Forcite module with the Condensed-phase Optimized Molecular Potentials for Atomistic Simulation Studies (COMPASS) force field. The convergence level for optimization was set to be ultrafine. For **P7** and **P15**, after the simulated single chains in melt state (at 473K) were relaxed to equilibrium, the distance between two carbons on the backbone that connect the two adjacent side-chains (R_{rep}) was measured.

Simulation of the molecular packing in CrE of **P2**, K_X of **P7** and Col_R of **P15**, was performed based on the XRD, FT-IR and EDM results. For example, the EDM of **P7** we finally chose suggested the approximate locations of biphenyls and carbonyls, and polarized FT-IR suggested that the polyethylene backbone was parallel to the *c*-axis. With these infromation, we manually placed the different components of **P7** in the unit cell with the possible symmetry of *Pnn*2. Afterwards, to obtain the optimized molecular packing, a supercell with *P*1 symmetry was needed for carrying out Geometry optimization, Anneal and Dynamics calculation. During simulation, the location of the biphenyls was carefully tuned and then fixed to ensure that the simulation could run based on the EDM results. After optimization, we compared the simulated diffraction pattern to the experimental data. It was found that the simulated diffraction pattern was sensitive to the array of different components of **P7** molecules in the unit cell. Therefore, to match the simulated diffraction as far as possible to the experimental observation, fine adjustment was necessary to be carried out. The possible molecular packing scheme and the conformation of chains in CrE, K_X and Col_R were obtained when the simulated and experimental diffractions reasonably agreed with each other.

Tables

Table S1. X-ray data of CrE in **P2**.

(hkl) plane	***q* (nm^{-1})**		***d*-spacing (nm)**	
	expt[a]	calcd[b]	expt[a]	cacld[b]
001	2.831	2.830	2.219	2.220
002	5.665	5.660	1.109	1.110
003	8.493	8.491	0.740	0.740
004	11.33	11.32	0.555	0.555
110	14.08	14.15	0.446	0.444
200	16.06	16.11	0.391	0.390
210	19.75	19.87	0.318	0.316

[a] Experimental values observed in Figure 1. [b] Calculated values based on the orthorhombic unit cell of a = 0.78 nm, b = 0.54 nm, c = 2.22 nm, $\alpha = \beta = \gamma$ = 90°.

Table S2. X-ray data of K_X in **P7**.

(hkl) plane	***q* (nm^{-1})**		***d*-spacing (nm)**		**intensity**	
	expt[a]	calcd[b]	expt[a]	cacld[b]	expt[c]	simu[d]
101	5.273	5.293	1.192	1.187	1.37	1.16
002	7.203	7.203	0.872	0.872	9	33.72
103	11.47	11.50	0.548	0.546	8.05	7.98
112	11.41	11.36	0.551	0.553	9.79	8.32
301	12.08	12.17	0.520	0.516	15.29	12.1
004	14.41	14.44	0.436	0.435	1.38	1.78
310	14.14	14.04	0.444	0.447	37.6	40.2
400	15.53	15.51	0.405	0.405	26.5	26.5
114	16.85	16.89	0.373	0.372	-	-
213	15.21	15.47	0.413	0.406	-	-
312	15.98	15.83	0.393	0.397	-	-
220	17.31	17.51	0.363	0.359	7.62	8.34
006	21.41	21.67	0.293	0.290	2.64	1.82

[a] Experimental values observed in Figure 2a. [b] Calculated values based on the orthorhombic unit cell of a = 1.62 nm, b = 0.80 nm, c = 1.74 nm, $\alpha = \beta = \gamma = 90°$. [c] Intensities observed from XRD experiment. [d] Simulated intensities estimated from molecular simulation. The intensities are classified as the exact numbers of integral areas. The experimental and simulated intensities of (400) are set to the same. Note that although the diffractions listed in the table satisfy the condition of $h + k + l = 2n$, the structure would not be body-centered because the polyethylene backbones pass though the unit cell along the c-axis and there exist the uncertainty of the packing of carbonyl groups and spacers.

Table S3. X-ray data of **P15**.

(hkl) plane	***q* (nm^{-1})**		***d*-spacing (nm)**	
	expt[a]	calcd[b]	expt[a]	cacld[b]
Low angle region				
010	3.466	3.471	1.812	1.810
020	6.966	6.943	0.902	0.905
030	10.40	10.41	0.604	0.603
100	4.936	4.947	1.273	1.270
001	3.852	3.855	1.631	1.630
110	6.032	6.042	1.042	1.040
High angle region				
~0.43 nm (hexagonal packing diffraction)				

[a] Experimental values observed in Figure 2b. [b] Calculated values based on the orthorhombic unit cell of a = 1.27 nm, b = 1.81 nm, c = 1.63 nm, $\alpha = \beta = \gamma = 90°$. The indexes are based on the assumption that the scattering *4′* reflected an additional density fluctuation perpendicular to both the *a*- and *b*-axis of Col$_R$, the diffraction/scattering *1′*, *2′*, *3′*, *4′* shown in Fig. 2b are assigned as (001), (100), (110) and (010), respectively.

Table S4. Number-average distance between two carbons on the backbone that connect the two adjacent side-chains ($<R_{\text{rep}}>$) of **P7** and **P15** in melt state (at 473K).

	P7		**P15**	
	$<R_{\text{rep}}>$ (nm)	**Standard deviation (nm)**	**$<R_{\text{rep}}>$ (nm)**	**Standard deviation (nm)**
Run *1*[a]	0.76	0.08	1.17	0.36
Run *2*[a]	0.74	0.06	1.16	0.33
Run *3*[a]	0.78	0.10	1.12	0.36
Overall[b]	0.76	0.09	1.15	0.35

[a] We created three independent single chains for each **P*n*** using Materials Studio. Once the single chain containing 30 repeating units was built, Geometry optimization was carried out to optimize the current structure. Afterwards, Anneal calculations were utilized to remove any thermal history (100 annealing cycles, optimize after each cycle), and then Dynamics calculation was carried out to obtain the final chain conformation. The data of $<R_{\text{rep}}>$ and the standard deviation for Run *1*, *2* and *3* were calculated using the R_{rep}s measured manually for the 30 repeating units of the chain obtained. As shown in the table, the three runs gave the similar $<R_{\text{rep}}>$s, suggesting that after Geometry optimization, Anneal and Dynamic calculation the single chains were relaxed to equilibrium. [b] We used the R_{rep}s of the 90 repeating units (= 3×30) to calculate the overall $<R_{\text{rep}}>$.

Figures

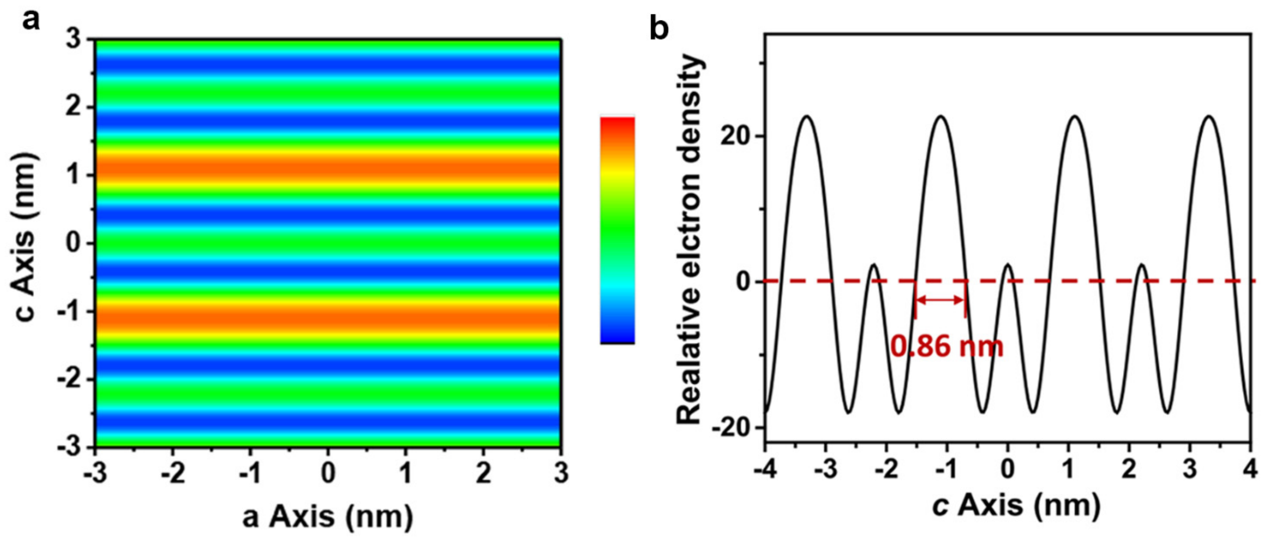

Fig. S1. (a) Reconstructed 2D electron density map (EDM) of the smectic-like layered structure of **P2**. The EDM was calculated based on the four low angle diffractions with the *q*-ratio of 1:2:3:4 in the 1D XRD profile. The phases of the four diffractions are selected to be -, +, - and -. Note that the *c*-axis is along the layer normal. (b) Variation of relative electron density along the normal of smectic-like layer in the CrE structure (i.e., the *c*-axis in (a)). According to (b), the mesogen layer is ~0.86 nm thick, corresponding to the length of biphenyl. This suggests that the biphenyls are fully interdigitated packed together (see Fig. S2).

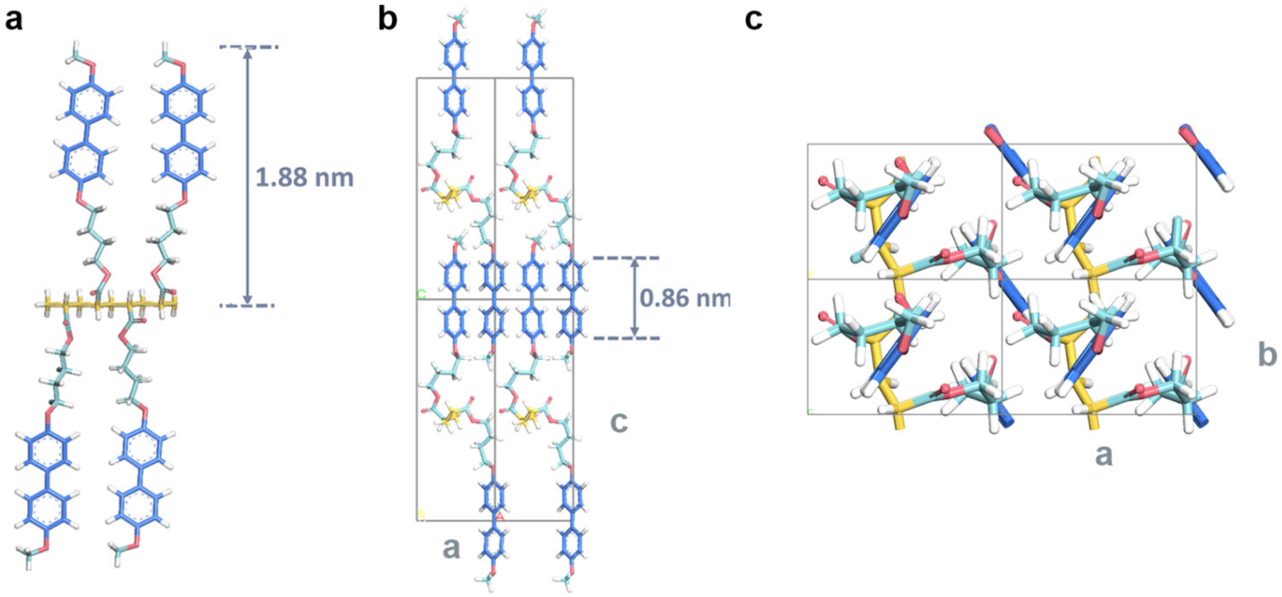

Fig. S2. (a) The extended side-chain length measured from the carbon on the backbone to the carbon on the methoxy end group. (b) Possible molecular packings of **P2** in CrE viewed along *b*-axis. The biphenyl groups emanating from the adjacent main-chain layers interdigitated pack together, forming the mesogen layer with the highest electron density. (c) Top view of the herringbone array of biphenyl mesogens.

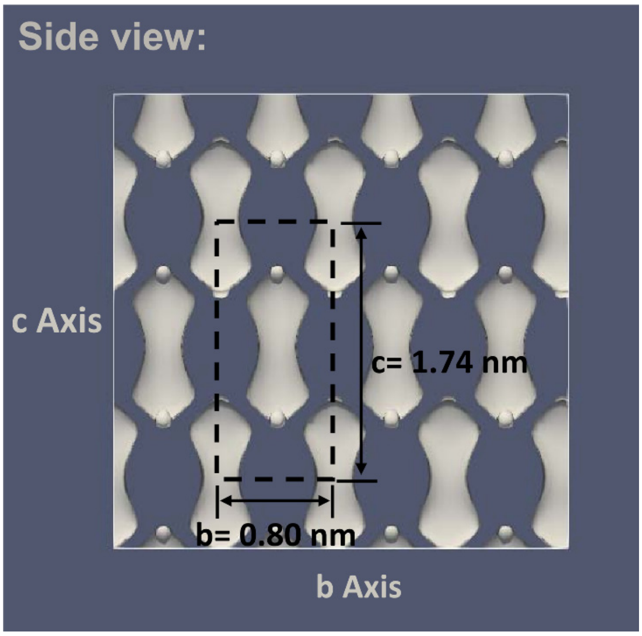

Fig. S3. Reconstructed 3D electron density map (EDM) of K_X of **P7** viewed along *a*-axis. The 3D EDM was calculated using the seven diffractions of (101), (002), (112), (103), (301), (310), (400) in the 1D XRD profile after corrected by subtracting the amorphous scattering, with the phases of +, +, -, -, -, + and +, respectively. The original structure for 3D Fourier transformation is orthorhombic. The display box size is 3.2 nm × 3.2 nm × 3.2 nm. In order to select the proper phases for the (*hkl*) diffractions, we used a trial-and-error approach. All the possible phase combinations were used to reconstruct the EDMs. For **P7**, the biphenyl group and the carbonyl group connected to the 7th carbon have the electron densities higher than the aliphatic component. So the "correct" map was selected based on the size of the highest electron density region representing the location of biphenyls and the volume fraction of the aliphatic component as well. Finally, their approximate locations in the K_X unit cell are shown in the 3D EDM.

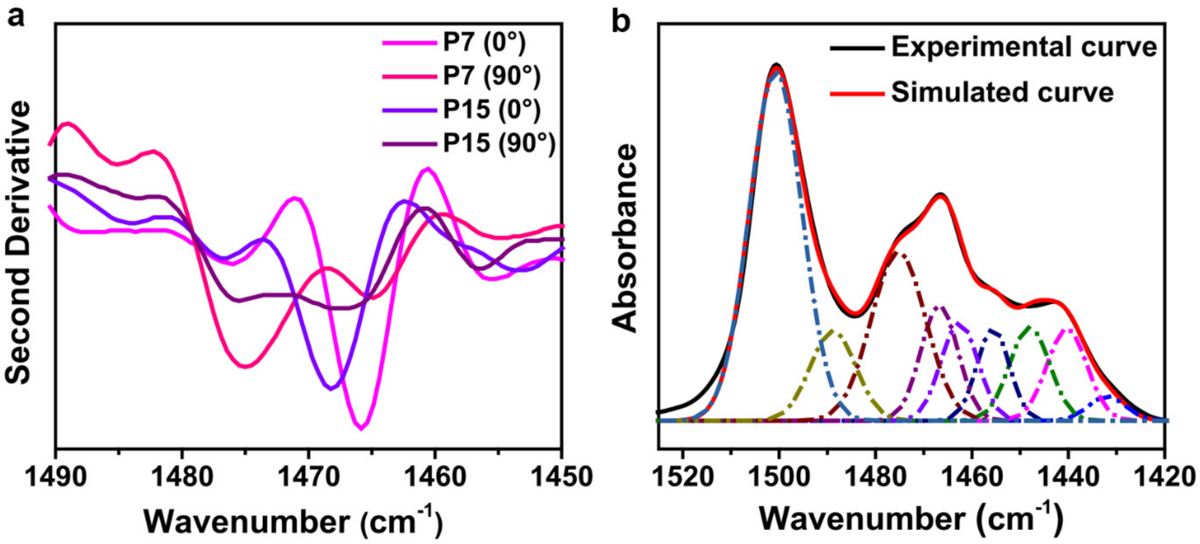

Fig. S4. (a) Second derivative curves of the polarized FT-IR results of **P7** and **P15**. (b) FT-IR results of the oriented **P7** without polarizer. With the aid of the second derivative of the FT-IR curve, the absorption band positions were identified, which were used in curve fitting (the dashed lines in (b)). In (b), the absorption band at 1475 cm^{-1} corresponds to *trans*-dominant conformation of methylene sequence, while that at 1468 cm^{-1} corresponds to *gauche*-dominant conformation.

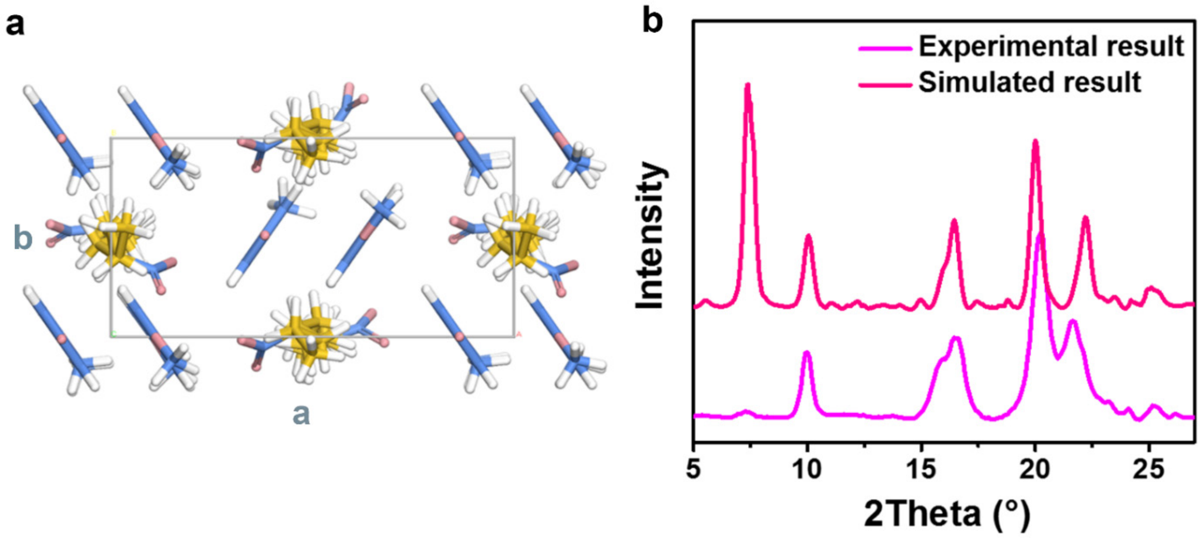

Fig. S5. (a) Top view of possible molecular arrangements of **P7** in K_X (projection along the *c*-axis). (b) Comparison of experimental and simulated 1D XRD profiles. Using Materials Studio, the simulated diffraction profile was calculated based on the molecular packing shown in (a) and Fig. 4b, which is in agreement with the experimental result except the one of (101). The calculated density of the simulated structure is 1.15 g/cm^3, very close to the experimentally measured one (1.14 g/cm^3). The space group of K_X could be *Pnn2*. We presume that the disagreement between experimental and simulated XRD results is due to that in K_X phase the molecular packing **P7** has some intrinsic defects and disordered conformations. Because of the tacticity was uncontrolled, the carbonyl at the 7th carbon may have different orientations in K_X, and thus do not have the exact positional order. The side-chain spacers may have different conformations. Such defects were not considered during the simulation. Namely, when simulating the diffractions, a perfect crystalline structure was assumed.

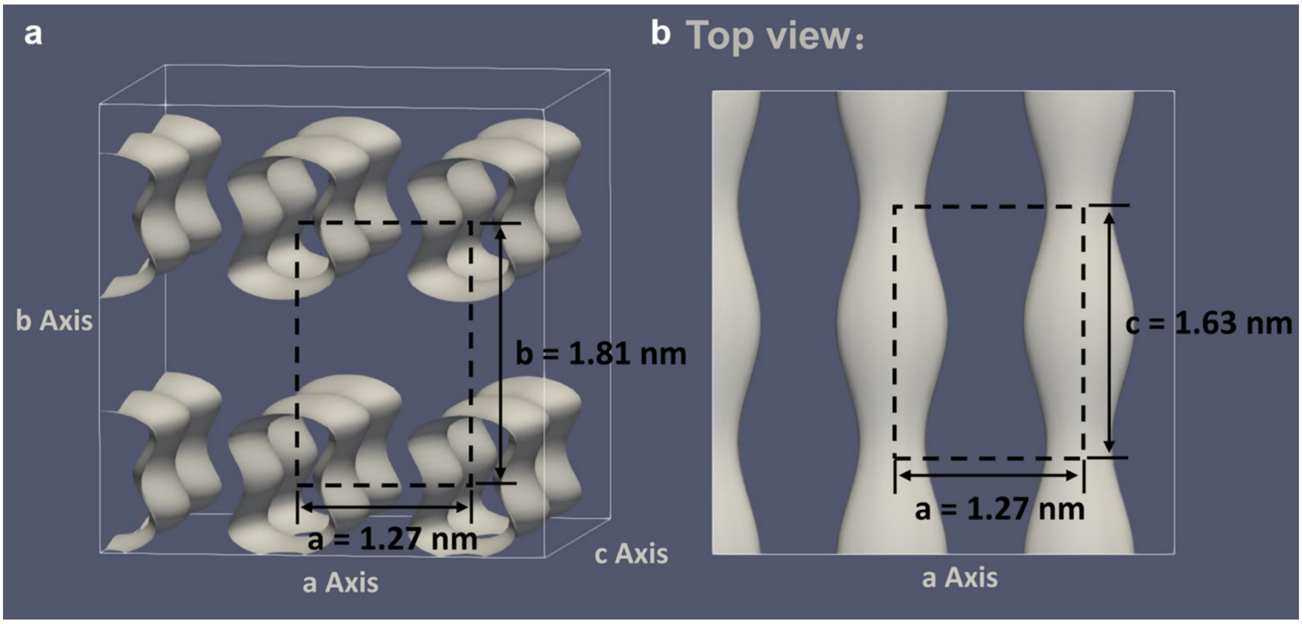

Fig. S6. (a) Reconstructed 3D electron density map (EDM) of **P15**. (b) 3D EDM result viewed along *b*-axis. As indicated in Fig. 3b, a diffusive and weak scattering appears at *4′*. Assuming that the scattering *4′* reflected an additional density fluctuation perpendicular to both the *a*- and *b*-axis of $\mathrm{Col_R}$, the diffraction/scattering *1′*, *2′*, *3′*, *4′* shown in Fig. 3b can thus be assigned as (010), (100), (110) and (001), respectively. Based on this assumption, the 3D EDM shown in this figure was calculated. The phases of the four diffractions/scatterings were selected to be +, -, + and -, respectively. The “correct” map was selected based on the size of the highest electron density region representing the location of biphenyls and the volume fraction of the aliphatic component. The original structure for 3D Fourier transformation is orthorhombic. The result suggests that the columns in $\mathrm{Col_R}$ may be undulated. The display box size is 3.2 nm × 3.2 nm × 3.2 nm.

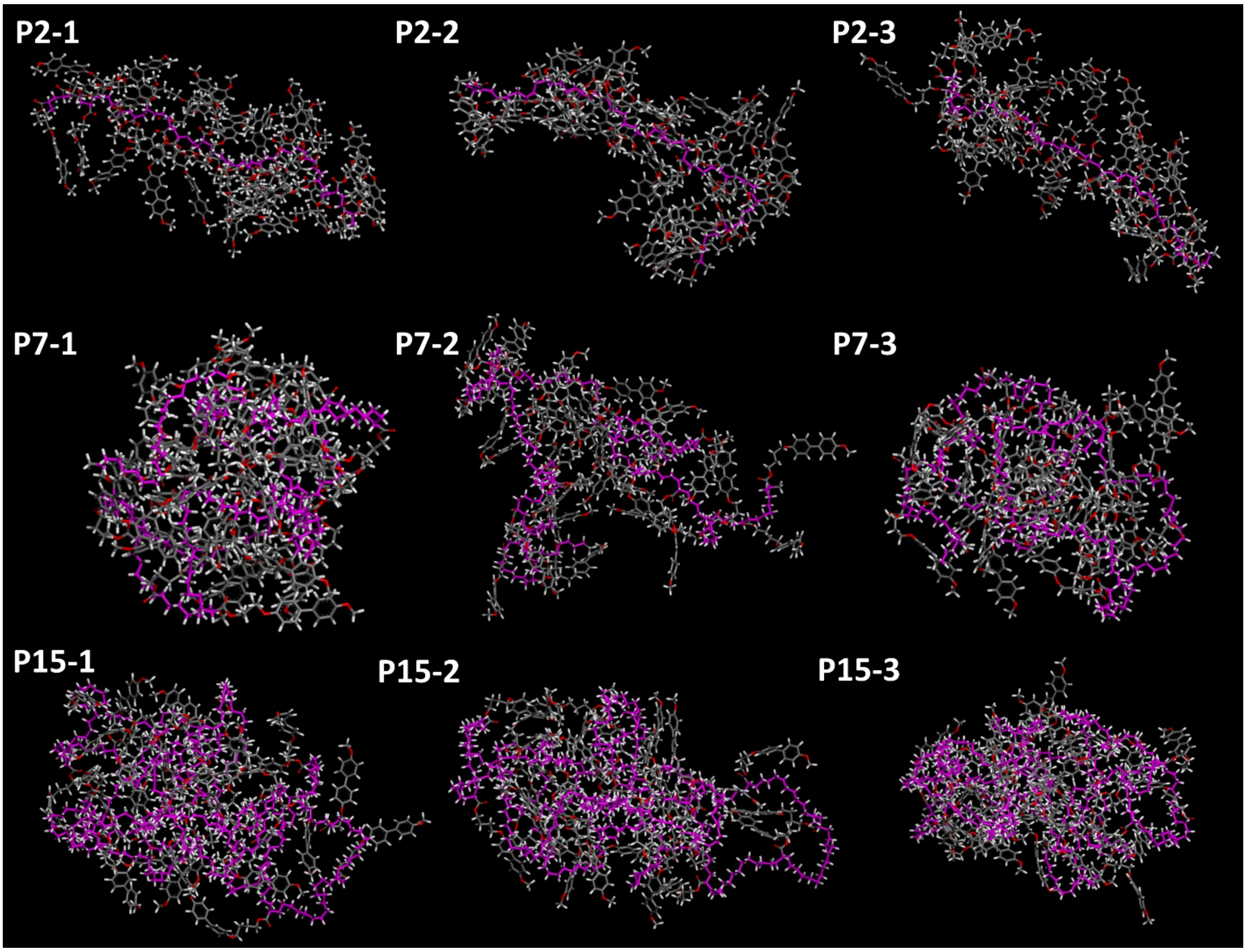

Fig. S7. Snapshots of the single chains of **P*n***s (30 repeating units) at melt state (at 473K) after the chains were relaxed to equilibrium. For each polymer, three independent simulations were run. The backbone is highlighted by pink color. It is found that **P2** backbone is quite extended, while **P7** and **P15** are more like random coil as a whole.

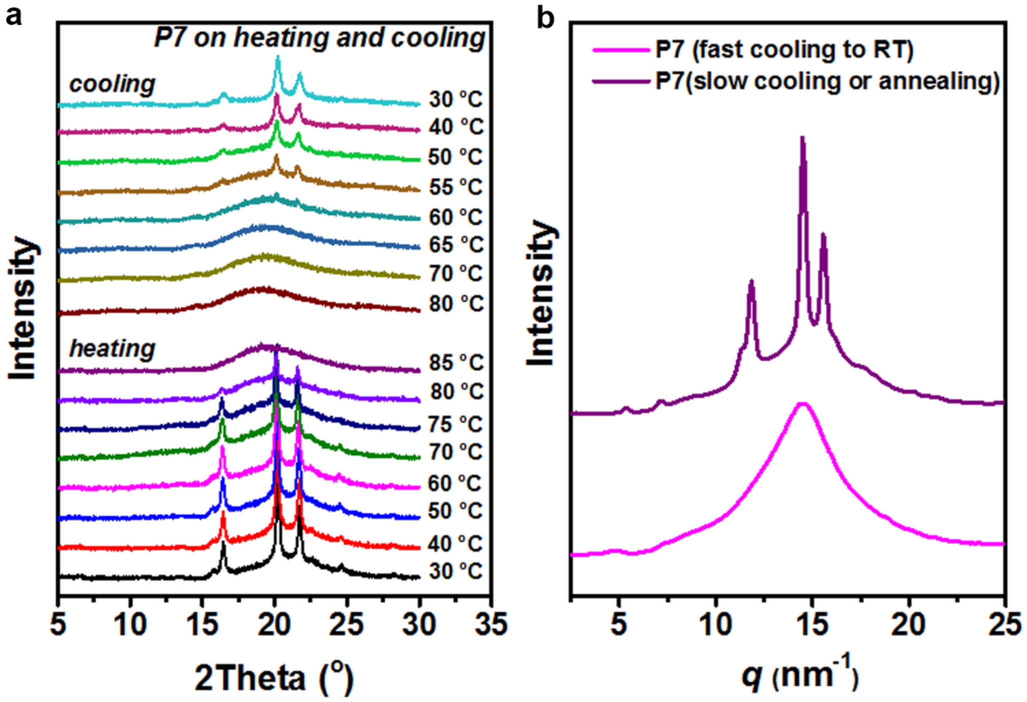

Fig. S8. (a) Thermal 1D XRD results of **P7** recorded upon heating and cooling. (b) 1D XRD profiles of **P7** recorded right after fast cooling from melt to RT (pink line), and after slow cooling to RT or thermal annealing at 63 °C for 1h (dark violet line).

Synthesis and Molecular Characterization

Scheme S1. Synthetic routes of **M15** and **P15**.

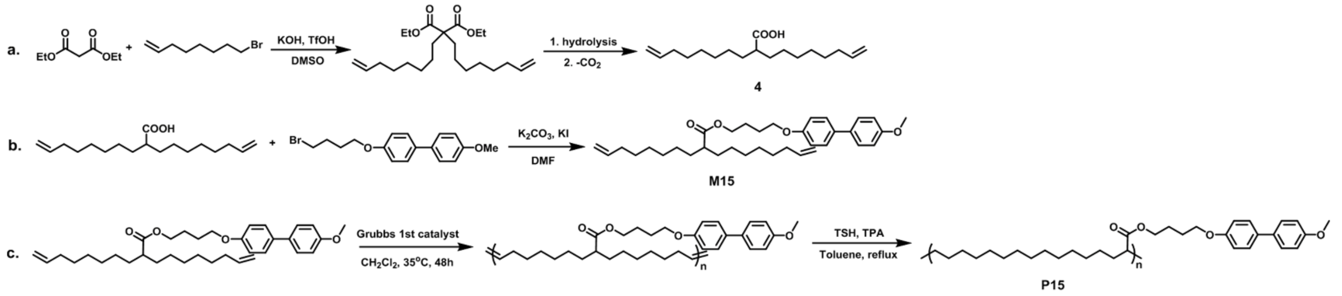

Scheme S2. Synthetic routes of **M2** and **P2**.

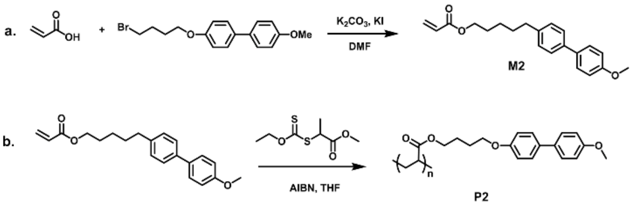

2-(3-Buten-1-yl)-5-hexenoic acid (1)

To a 250 mL three-necked, round-bottom flask was added potassium hydroxide (14.7 g, 262 mmol) and anhydrous DMSO (60 mL) under nitrogen purge. Trifluoromethanesulfonic acid (16.9 g, 113 mmol) was slowly dropped into system at 0 °C. 4-Bromo-1-butene (11 g, 82.1 mmol) and diethyl malonate (6 g, 37.5 mmol) were added successively at room temperature, and the resulting mixture was stirred at 65 °C overnight. After the reaction was finished, the mixture was diluted with ethyl acetate, and washed with 1M hydrochloric acid, saturated $NaHCO_3$ aqueous solution, and brine. The combined organic layers were concentrated.

To a 100 mL round-bottom flask were added the residue in the last procedure, KOH (16 g, 285 mmol), ethanol (30 mL), deionized water (5 mL). The mixture was refluxed for 24 h. 1M hydrochloric acid was slowly added into the reaction mixture until the pH of the system was about 2~3. The resulting mixture was diluted with ethyl acetate, and washed with brine. The organic layers were dried with anhydrous sodium sulfate and concentrated.

To a 100 mL round-bottom flask were added the residue in the last procedure, LiCl (9.5 g, 225 mmol), DMSO (30 mL), deionized water (5 mL). The mixture was heated to 150 °C for 24 h. After the reaction was finished, the resulting mixture was diluted with ethyl acetate, and washed with brine. The organic layers were dried with anhydrous sodium sulfate and concentrated. The residue was purified by column chromatography by using the eluent of petroleum ether and dichloromethane (1:1). **2-(3-buten-1-yl)-5-hexenoic acid (1)** was obtained as colorless oil in yield of 68%. **^{1}H NMR** (400 MHz, $CDCl_3$, δ, ppm): 11.97 (s, 1H), 5.79 (ddt, *J* = 16.8 Hz, 10.0, 6.6, 2H), 5.01 (dd, *J* = 22.6 Hz, 13.7 Hz, 4H), 2.52 – 2.34 (m, 1H), 2.19 – 2.00 (m, 4H), 1.77 (td, *J* = 14.5 Hz, 8.4 Hz, 2H), 1.59 (ddd, *J* = 14.0 Hz, 8.7 Hz, 6.2 Hz, 2H).

4'-Methoxy[1,1'-biphenyl]-4-ol (2)

1,4-Bromophenol (3.0 g, 17.3 mmol), (4-methoxyphenyl)boronic acid (2.29 g, 19.1 mmol), Pd/C (10 wt% on carbon, 300 mg), K_2CO_3 (9.58 g, 69.4 mmol), and deionized water (40 mL) were added to 100 mL round-bottom flask at 0 °C. Then the reaction system was warmed to room temperature and stirred for 24 h. After the reaction was finished, an aqueous solution of HCl (40 mL, 1M) was added to quench the reaction. The resulting mixture was filtered and the insoluble part was washed with acetone twice. The filtrate was washed with dichloromethane three times. The combined organic layers were evaporated to yield a white residue. Then the residue was purified by column chromatography using CH_2Cl_2 as eluent to obtain white solid **2** (3.46 g, in 72%). **^{1}H NMR** (400 MHz, $CDCl_3$, δ, ppm): 7.43 (t, *J* = 8.9 Hz, 4H), 6.91 (dd, *J* = 26.3 Hz, 8.6 Hz, 4H), 3.84 (s, 3H).

4-(4-Bromobutoxy)-4'-methoxy-1,1'-biphenyl (3)

1,4-Dibromobutane (15 g, 69.5 mmol), K_2CO_3 (7.2 g, 52.1 mmol), a catalyst amount of KI and acetone (150 mL) were added into a 250 mL three-necked round-bottom flask. A solution of **2** (3.46 g, 17.3 mmol) in acetone (50 mL) was dropped slowly into the system. The mixture was refluxed until **2** was completely exhausted by TLC analysis. The reaction mixture was immediately filtrated to remove the insoluble salt after the reaction was finished and concentrated *in vacuo*. The residue was purified by column chromatography (petroleum ether: dichloromethane, 1:1) to yield white solid **3** (5.8 g, in 78% yield). **^{1}H NMR** (400 MHz, $CDCl_3$, δ, ppm): 7.47 (dd, *J* = 8.6 Hz, 2.9, 4H), 6.95 (t, *J* = 8.0 Hz, 4H), 4.03 (t, *J* = 5.9 Hz, 2H), 3.84 (s, 3H), 3.50 (t, *J* = 6.6 Hz, 2H), 2.17 – 2.04 (m, 2H), 2.02 – 1.88 (m, 2H); **^{13}C NMR** (100 MHz, $CDCl_3$, δ, ppm): 158.71, 157.98, 133.56, 133.46, 127.76, 127.75, 114.72, 114.18, 66.91, 55.37, 33.54, 29.51, 27.95.

2-(3-Buten-1-yl)-5-hexenoic acid, 4'-(methoxy)[1,1'-biphenyl]-4-yl ester (M7)

1 (0.8 g, 4.76 mmol), 3 (1.75 g, 5.22 mmol), K_2CO_3 (1.97 g, 14.3 mmol), a catalyst amount of KI and anhydrous DMF (20 mL) were added into a 50 mL round-bottom flask. The mixture was heated to 100 °C overnight. After the reaction was finished, the resulting mixture was diluted with ethyl acetate and washed with brine three times. The organic layer was concentrated *in vacuo* and purified by column chromatography (petroleum ether: dichloromethane, 1:1). White solid product **M7** was obtained in a yield of 85%. **^{1}H NMR** (400 MHz, $CDCl_3$, δ, ppm): 7.47 (dd, *J* = 8.4 Hz, 3.8 Hz, 4H), 6.95 (t, *J* = 7.3 Hz, 4H), 5.85 – 5.67 (m, 2H), 4.99 (dd, *J* = 19.2 Hz, 13.7 Hz, 4H), 4.17 (t, *J* = 5.7 Hz, 2H), 4.03 (t, *J* = 5.3 Hz, 2H), 3.84 (s, 3H), 2.49 – 2.34 (m, 1H), 2.17 – 2.00 (m, 4H), 1.87 (s, 4H), 1.81 – 1.70 (m, 2H), 1.55 (td, *J* = 13.8 Hz, 7.1 Hz, 2H). **^{13}C NMR** (100 MHz, $CDCl_3$, δ, ppm): 176.01, 158.73, 158.00, 137.86, 133.50, 127.74, 115.15, 114.74, 114.16, 67.36, 63.92, 55.37, 44.49, 31.56, 31.54, 26.00, 25.57. **HRMS (ESI):** m/z calcd for $C_{27}H_{34}O_4 + H^+$: 423.25 $[M+H]^+$; found: 423.2529. **Elemental analysis:** calcd (%) for $C_{27}H_{34}O_4$: C 76.74, H 8.11, O 15.14; found: C 76.75, H 8.26, O 14.99.

Polymerization of M7 and hydrogenation

M7 (300 mg, 0.71 mmol) was added into a dry Schlenk tube equipped with a magnetic stirring bar. After three pump-purge cycles with nitrogen, anhydrous DCM (200 µL) was injected to fully dissolve the monomer. Then the Grubbs 1st generation catalyst was added under vigorous stirring. The by-product ethylene was removed by successive nitrogen purge, and the reaction temperature was kept at 35 °C. After 48 h, a few drops of vinyl ethyl ether were added to the system to quench the polymerization. The resulting mixture was diluted with THF (2 mL) and dropped to methanol (50 mL) under stirring. The dissolution and precipitation process were repeated three times to remove catalyst. Then the resulting unsaturated polymer was collected by centrifugation, and dried under vacuum at 40 °C as brown solid in a yield of 92%. **^{1}H NMR** (400 MHz, $CDCl_3$, δ, ppm): 7.44 (d, *J* = 5.5 Hz, 4H), 6.91 (d, *J* = 8.1 Hz, 4H), 5.33

(d, *J* = 13.9 Hz, 2H), 5.04 – 4.91 (m, 1H), 4.12 (s, 2H), 4.00 (d, *J* = 20.5 Hz, 2H), 3.83 (d, *J* = 12.6 Hz, 3H), 2.33 (s, 1H), 1.94 (s, 4H), 1.82 (s, 4H), 1.65 (s, 2H), 1.47 (s, 2H).

The unsaturated polymer (250 mg, 0.63 mmol double bond) obtained in the last procedure, benzenesulfonic acid (387 mg, 2.08 mmol), tripropylamine (361 mg, 2.52 mmol) and dry toluene (10 mL) were added into a 20 mL round-bottom flask. The mixture was refluxed for 24 h. After cooling to room temperature, the reaction mixture was washed with water, dried by anhydrous Na_2SO_4, and concentrated in vacuo. The residue was dissolved in THF (2 mL) and dropped into methanol (50 mL). After centrifugation, polymer **P7** was obtained as a white solid (204 mg, in 82% yield). **^{1}H NMR** (400 MHz, $CDCl_3$, δ, ppm): 7.44 (dd, *J* = 8.6 Hz, 4.7 Hz, 4H), 6.92 (t, *J* = 8.5 Hz, 4H), 4.13 (d, *J* = 6.0, 2H), 3.98 (t, *J* = 5.0 Hz, 2H), 3.82 (d, *J* = 6.1 Hz, 3H), 2.34 – 2.22 (m, 1H), 1.82 (s, 4H), 1.55 (s, 3H), 1.22 (s, 8H).

Since **M15** and **P15** was synthesized similarly to **M7** and **P7**, here we only list the molecular characterization results.

2-(7-Octen-1-yl)-9-decenoic acid (4)

4 was obtained as colorless oil in yield of 73%. **^{1}H NMR** (400 MHz, $CDCl_3$, δ, ppm): 11.64 (s, 1H), 5.93 – 5.62 (m, 2H), 4.96 (dd, *J* = 24.3 Hz, 13.6 Hz, 4H), 2.40 – 2.25 (m, 1H), 2.03 (q, *J* = 6.8 Hz, 4H), 1.49 (ddd, *J* = 33.1 Hz**,** 19.9 Hz, 6.4 Hz, 4H), 1.39 – 1.12 (m, 16H).

2-(7-Octen-1-yl)-9-decenoic acid, 4'-(methoxy)[1,1'-biphenyl]-4-yl ester (M15)

M15 was obtained as colorless oil in yield of 84%. **^{1}H NMR** (400 MHz, $CDCl_3$, δ, ppm): 7.47 (dd, *J* = 8.3 Hz, 4.0 Hz, 4H), 6.95 (t, *J* = 7.7 Hz, 4H), 5.89 – 5.67 (m, 2H), 4.95 (dd, *J* = 23.9 Hz, 13.6 Hz, 4H), 4.16 (t, *J* = 5.7 Hz, 2H), 4.01 (d, *J* = 5.6, 2H), 3.84 (s, 3H), 2.41 – 2.23 (m, 1H), 2.10 – 1.92 (m, 4H), 1.75 (d, *J* = 85.7 Hz, 4H), 1.59 – 1.15 (m, 20H). ^{13}C NMR (100 MHz, $CDCl_3$, δ, ppm): 176.53, 158.66, 157.98, 139.10, 133.55, 127.79, 114.67, 114.21, 114.01, 67.33, 63.72, 55.44, 45.79, 33.83, 32.27, 29.36, 28.99, 28.86, 27.46, 25.99, 25.58. **HRMS (ESI):** m/z calcd for $C_{35}H_{50}O_4 + H^+$: 535.37 $[M+H]^+$; found: 535.3781. **Elemental analysis:** calcd (%) for $C_{35}H_{50}O_4$: C 78.61, H 9.42, O 11.97; found: C 78.67, H 9.64, O 11.69.

Polymerization of M15 and hydrogenation

Unsaturated polymer was obtained as brown tacky solid in yield of 87%. **^{1}H NMR** (400 MHz, $CDCl_3$, δ, ppm): 7.54 – 7.40 (m, 4H), 6.93 (t, *J* = 8.1 Hz, 4H), 5.43 – 5.28 (m, 2H), 4.14 (s, 2H), 3.99 (d, *J* = 5.5 Hz, 2H), 3.82 (s, 3H), 2.30 (s, 1H), 1.95 (d, *J* = 16.5 Hz, 4H), 1.84 (s, 4H), 1.57 (s, 2H), 1.42 (s, 2H), 1.34 (d, 16H).

P15 was obtained as white solid in yield of 90%. **^{1}H NMR** (400 MHz, $CDCl_3$, δ, ppm): 7.53 – 7.43 (m, 4H), 6.93 (t, *J* = 8.1 Hz, 4H), 4.15 (t, *J* = 5.9 Hz, 2H), 4.00 (t, *J* = 5.6 Hz, 2H), 3.83 (s, 3H), 2.36 – 2.26 (m, 1H), 1.85 (s, 4H), 1.56 (dd, *J* = 16.6 Hz, 8.7 Hz, 4H), 1.22 (s, 24H).

2-Propenoic acid, 4-[(4'-methoxy[1,1'-biphenyl]-4-yl)oxy]butyl ester (M2)

M2 was prepared from propenoic acid and 3 by using the same method described in the preparation of **M7** in yield of 64%. **^{1}H NMR** (400 MHz, $CDCl_3$, δ, ppm): 7.47 (dd, *J* = 8.4 Hz, 4.0 Hz, 4H), 7.09 – 6.87 (m, 4H), 6.41 (d, *J* = 17.3 Hz, 1H), 6.13 (dd, *J* = 17.3 Hz, 10.4 Hz, 1H), 5.83 (d, *J* = 10.4 Hz, 1H), 4.26 (d, *J* = 5.4 Hz, 2H), 4.03 (s, 2H), 3.84 (s, 3H), 1.90 (s, 4H). **^{13}C NMR** (101 MHz, $CDCl_3$, δ, ppm): 166.00, 158.46, 155.45, 133.49, 132.11, 130.72, 129.40, 128.51, 127.95, 127.74, 120.63, 114.74, 114.45, 114.17, 112.01, 67.35, 64.23, 55.37, 25.95, 25.46. **HRMS (ESI)**: m/z calcd for $C_{20}H_{22}O_4 + H^+$: 327.16 $[M+H]^+$; found: 327.1590. **Elemental analysis**: calcd (%) for $C_{20}H_{22}O_4$: C 73.60, H 6.79, O 19.61; found: C 73.62, H 6.95, O 19.43.

Polymerization of M2

M2 (300 mg, 0.93 mmol), O-ethyl-S-(1-methoxycarbonyl)ethyldithiocarbonate (RAFT chain transfer agent, 1 mol%), AIBN (initiator, 0.33 mol%) and dry THF (1 mL) were added to a flame-dried polymerization tube. After the tube was dehydrated and deoxygenated by three freeze-pump-thaw cycles, the polymerization tube was sealed with gas fire. Then the reaction was conducted at 65 °C under vigorous stirring. After 24h, the tube was immersed into liquid nitrogen to quench the reaction. The resulting mixture was diluted with THF (2 mL), and dropped into methanol (50 mL). After centrifugation, polymer **P2** was obtained as a white solid (234 mg, in 78% yield). **^{1}H NMR** (400 MHz, $CDCl_3$, δ, ppm): 7.29 (d, *J* = 26.6 Hz, 5H), 6.91 (d, *J* = 69.2 Hz, 4H), 4.05 (d, *J* = 44.8 Hz, 2H), 3.98 – 3.83 (m, 2H), 3.83 – 3.70 (m, 3H), 2.32 (s, 1H), 1.68 (d, 6H).

NMR spectra of the monomers and polymers

M2 - ^{1}H

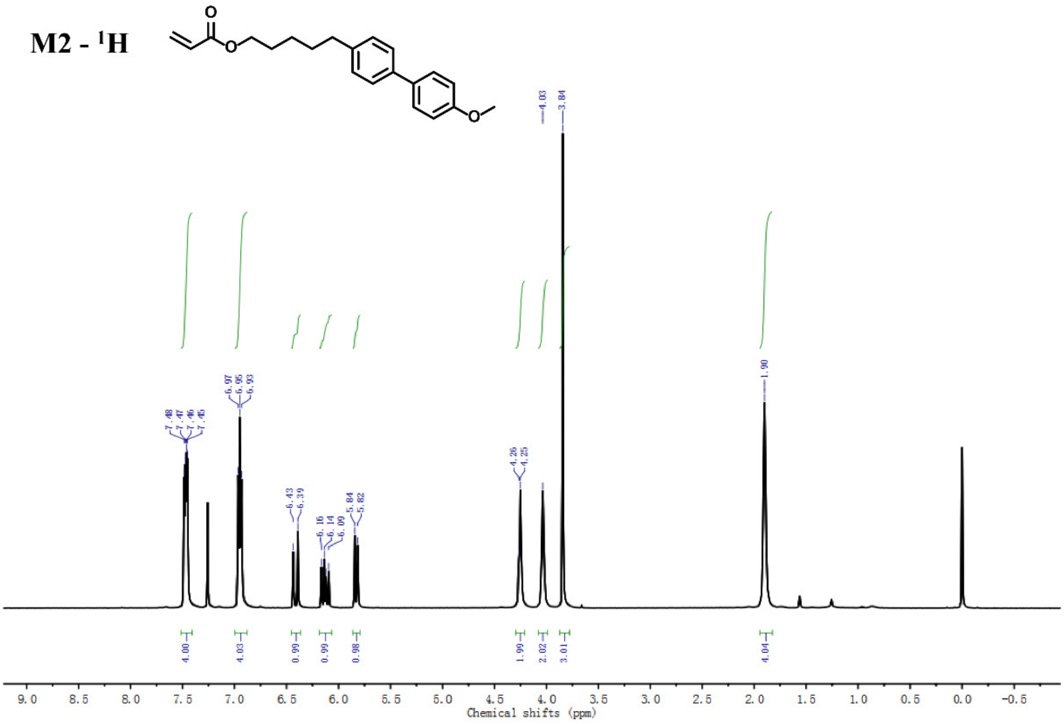

M2 - ^{13}C

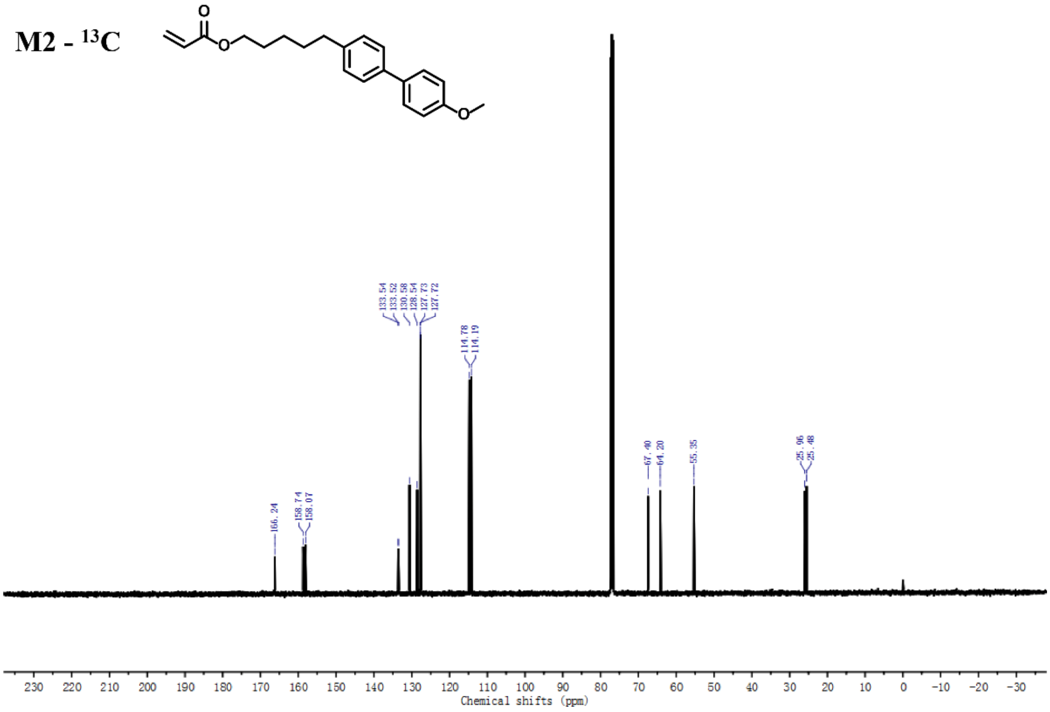

P2 - ^{1}H

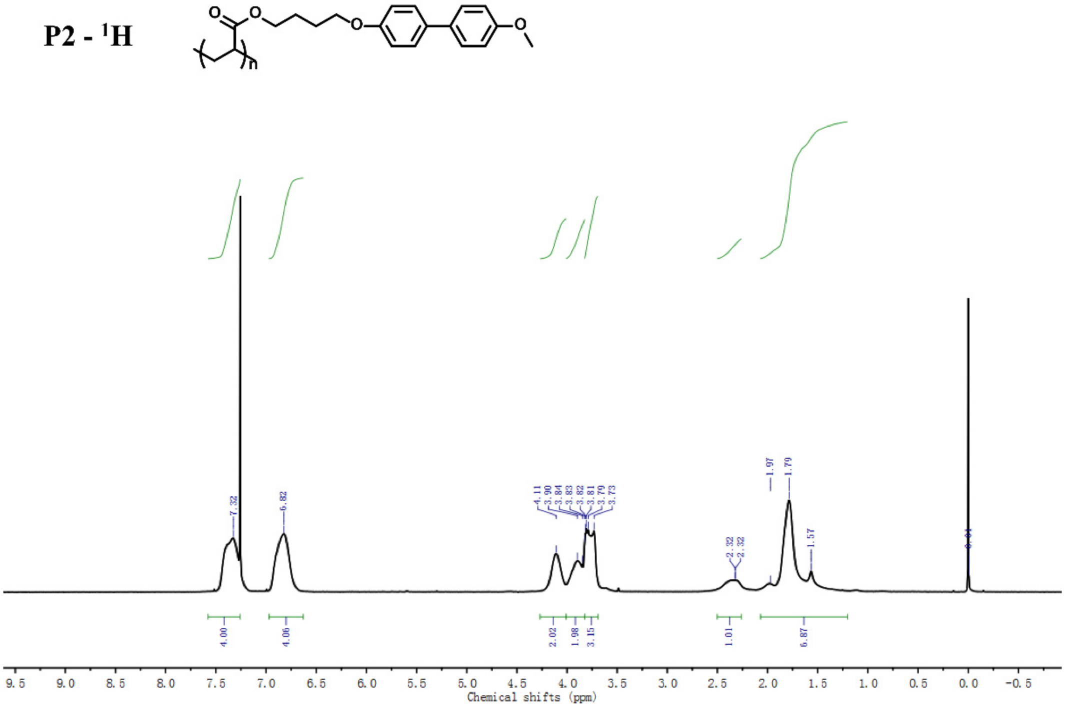
7.32
6.82
4.11
3.90
3.84
3.83
3.82
3.81
3.79
3.73
2.32
2.32
1.97
1.79
1.57
0.01
4.00
4.06
2.02
1.98
3.15
1.01
6.87
9.5 9.0 8.5 8.0 7.5 7.0 6.5 6.0 5.5 5.0 4.5 4.0 3.5 3.0 2.5 2.0 1.5 1.0 0.5 0.0 -0.5
Chemical shifts (ppm)

M7 - ^{1}H

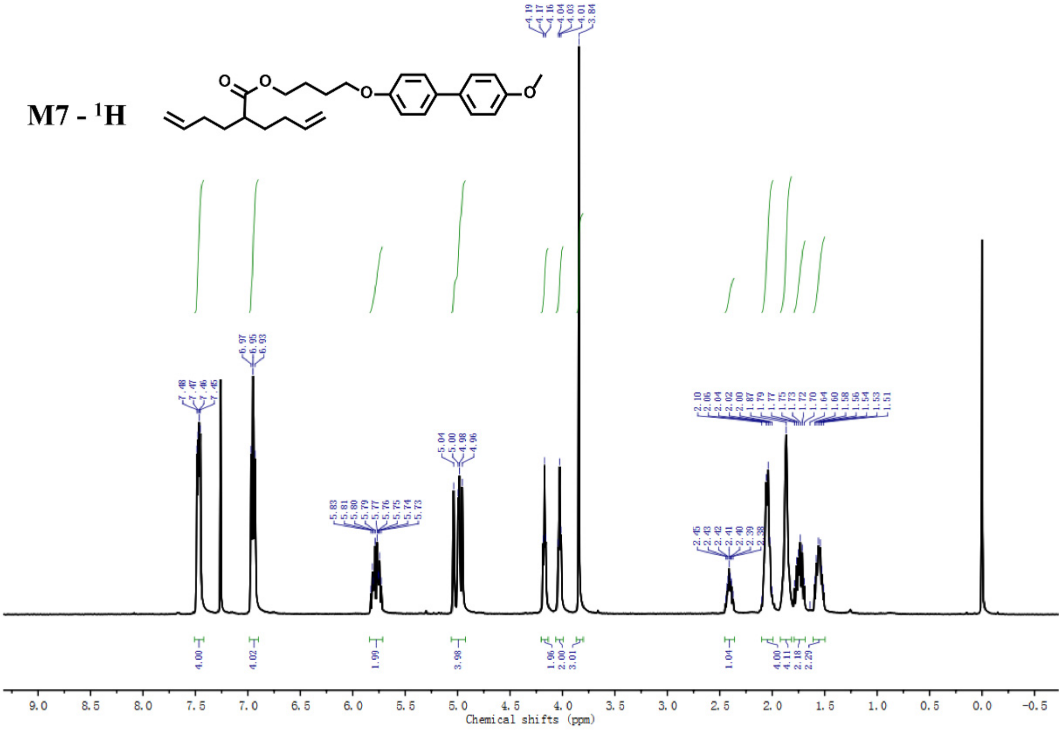
4.19
4.17
4.16
4.04
4.03
4.01
3.84
7.48
7.47
7.46
7.45
6.97
6.95
6.93
5.83
5.81
5.80
5.79
5.77
5.76
5.75
5.74
5.73
5.04
5.00
4.98
4.96
2.45
2.43
2.42
2.41
2.40
2.39
2.38
2.10
2.06
2.04
2.02
2.00
1.87
1.79
1.77
1.75
1.73
1.72
1.70
1.64
1.60
1.58
1.56
1.54
1.53
1.51
4.00
4.02
1.99
3.98
1.96
2.00
3.01
1.04
4.00
4.11
2.18
2.29
9.0 8.5 8.0 7.5 7.0 6.5 6.0 5.5 5.0 4.5 4.0 3.5 3.0 2.5 2.0 1.5 1.0 0.5 0.0 -0.5
Chemical shifts (ppm)

M7 - ^{13}C

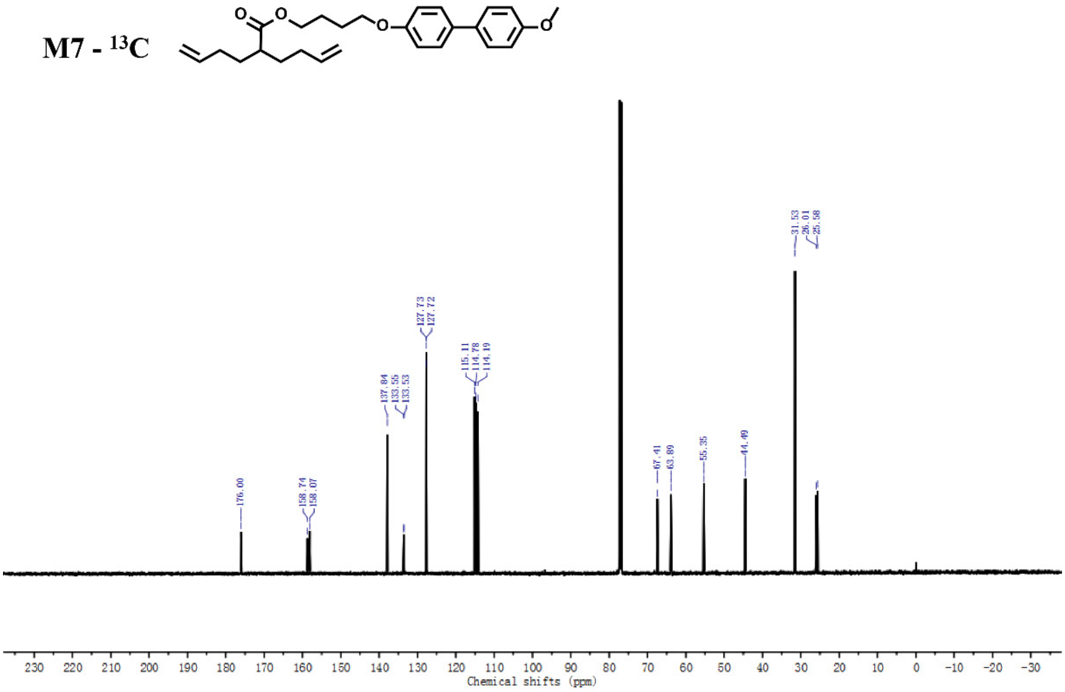

P7 before hydrogenation - ^{1}H

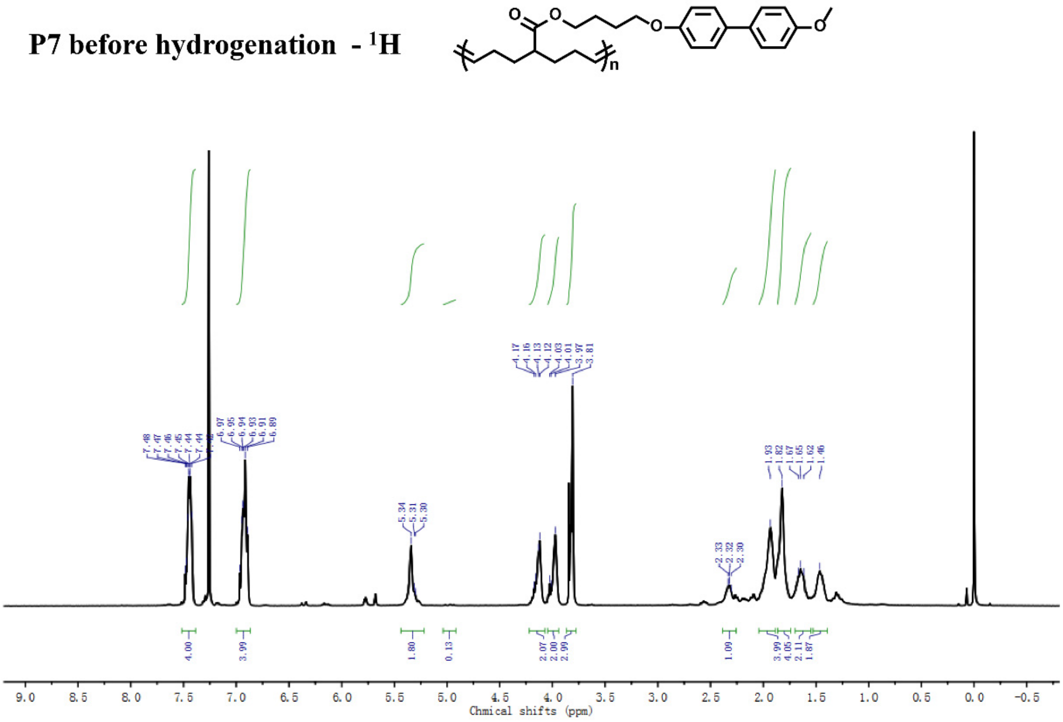

P7 - ^{1}H

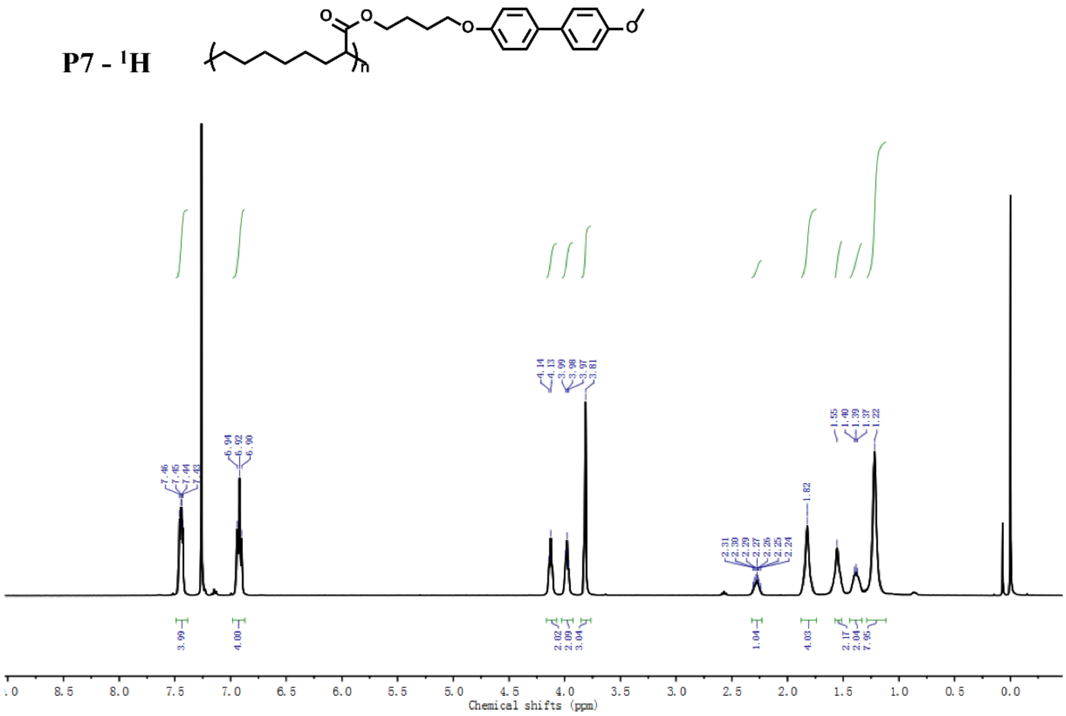

O
O
O
O
n
7.46
7.45
7.44
7.43
6.94
6.92
6.90
4.14
4.13
3.99
3.98
3.97
3.81
2.31
2.30
2.29
2.27
2.26
2.25
2.24
1.82
1.55
1.40
1.39
1.37
1.22
3.99
4.00
2.02
2.09
3.04
1.04
4.03
2.17
2.04
7.95
.0
8.5
8.0
7.5
7.0
6.5
6.0
5.5
5.0
4.5
4.0
3.5
3.0
2.5
2.0
1.5
1.0
0.5
0.0
Chemical shifts (ppm)

M15 - ^{1}H

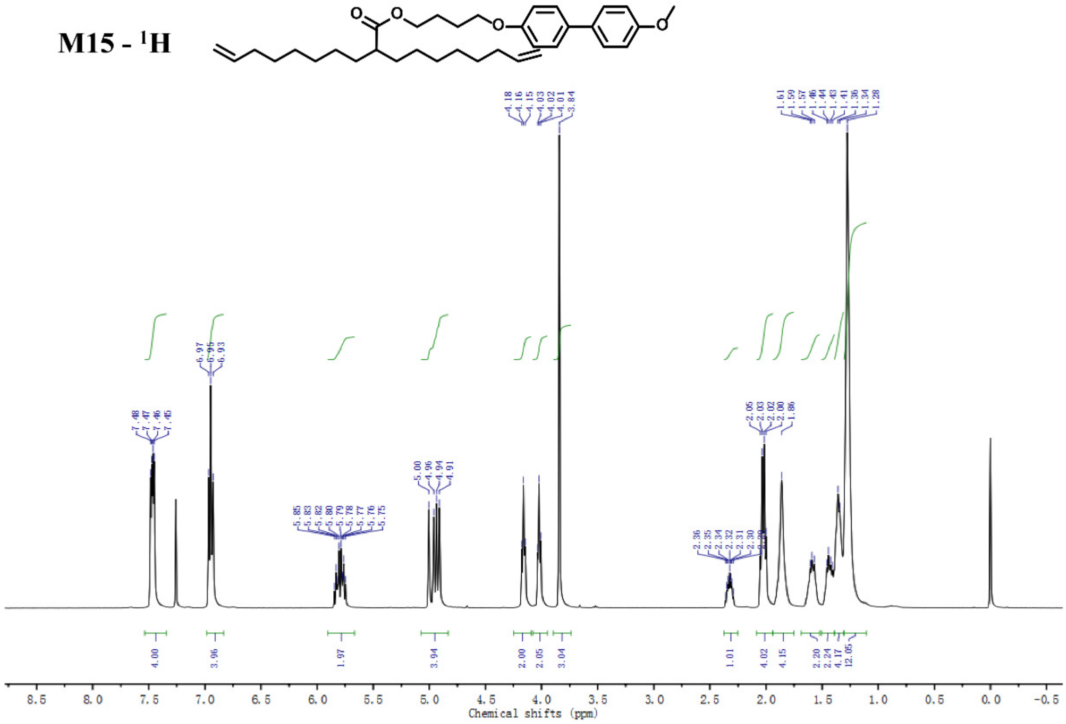

O
O
O
O
7.48
7.47
7.46
7.45
6.97
6.95
6.93
5.85
5.83
5.82
5.80
5.79
5.78
5.77
5.76
5.75
5.00
4.96
4.94
4.91
4.18
4.16
4.15
4.03
4.02
4.01
3.84
2.36
2.35
2.34
2.32
2.31
2.30
2.29
2.05
2.03
2.02
2.00
1.86
1.61
1.59
1.57
1.46
1.44
1.43
1.41
1.36
1.34
1.28
4.00
3.96
1.97
3.94
2.00
2.05
3.04
1.01
4.02
4.15
2.20
2.24
4.17
12.05
8.5
8.0
7.5
7.0
6.5
6.0
5.5
5.0
4.5
4.0
3.5
3.0
2.5
2.0
1.5
1.0
0.5
0.0
-0.5
Chemical shifts (ppm)

M15 - ^{13}C

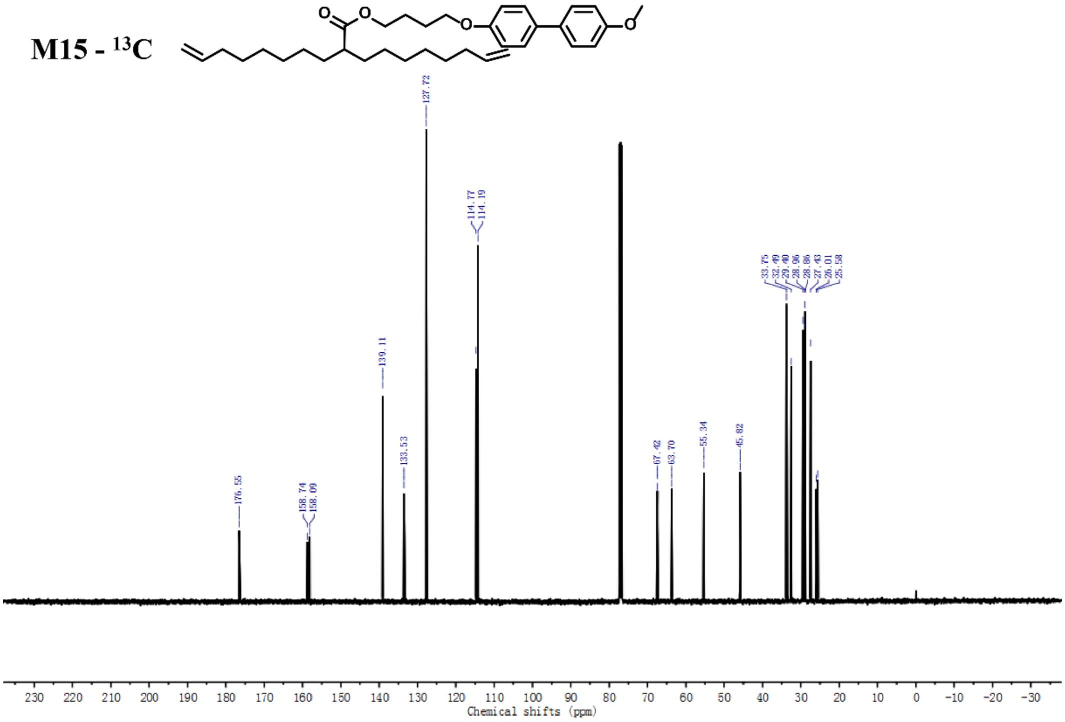

P15 before hydrogenation - ^{1}H

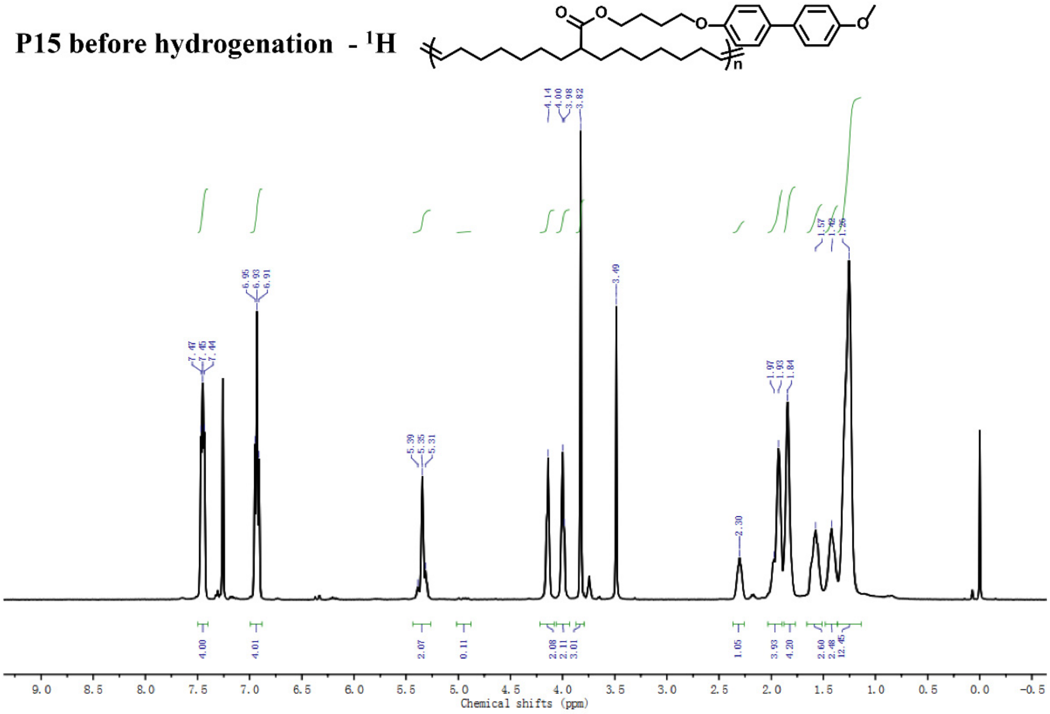

P15 - ^{1}H

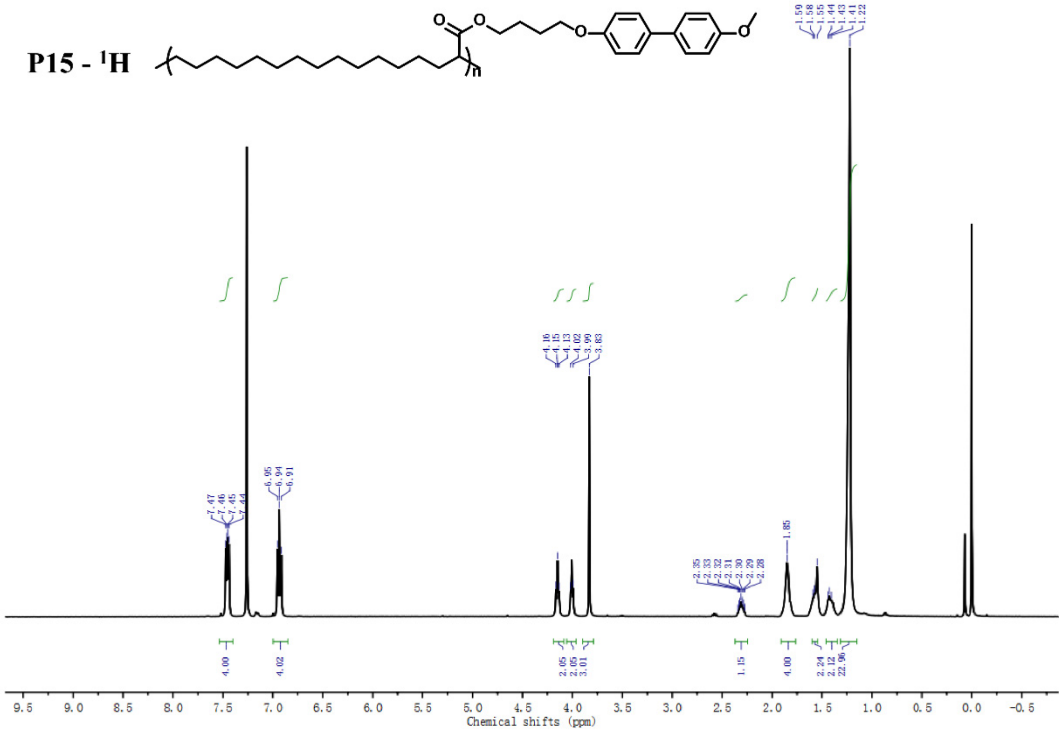
O
O
O
O
n
1.59
1.58
1.55
1.44
1.43
1.41
1.22
4.16
4.15
4.13
4.02
3.99
3.83
6.95
6.94
6.91
7.47
7.46
7.45
7.44
2.35
2.33
2.32
2.31
2.30
2.29
2.28
1.85
4.00
4.02
2.05
2.05
3.01
1.15
4.00
2.24
2.12
22.96
9.5
9.0
8.5
8.0
7.5
7.0
6.5
6.0
5.5
5.0
4.5
4.0
3.5
3.0
2.5
2.0
1.5
1.0
0.5
0.0
-0.5
Chemical shifts (ppm)